Earth and Space Science

Key Points:

- Integrated Multi-satellitE Retrievals for Global Precipitation Measurement (IMERG)-Final generally outperforms ERA5 and ERA5-Land
- ERA5 and ERA5-Land precipitation products have similar spatiotemporal patterns and ERA5-Land slightly outperforms ERA5
- ERA5 and ERA5-Land significantly overestimate the event duration and underestimate the mean event precipitation rate

Correspondence to:
M. Chen,
cmq12@jxau.edu.cn

Comprehensive Evaluations on the Error Characteristics of the State-of-the-Art Gridded Precipitation Products Over Jiangxi Province in 2019

Tulin Hong[1,2,3], Hongyi Li[4], and Meiqiu Chen[1,2]

[1]College of Land Resources and Environment, Jiangxi Agricultural University, Nanchang, China, [2]Jiangxi Province Key Laboratory of Poyang Lake Basin Agricultural Resources and Ecology, Nanchang, China, [3]Land Consolidation and Rehabilitation Center of Jiangxi, Nanchang, China, [4]Department of Land Resource Management, Jiangxi University of Finance and Economics, Nanchang, China

Abstract Accurate knowledge of the precipitation estimates with high quality and fine spatiotemporal resolutions is crucial to the precipitation science communities, especially over poorly gauged regions. In this study, we apply various validation metrics to comprehensively evaluate three latest model-based and satellite-based precipitation products, namely the fifth-generation global atmospheric analysis data set of the European Center for Medium-Range Weather Forecasts (ECMWF) (ERA5), ERA5-Land and Integrated Multi-satellitE Retrievals for Global Precipitation Measurement (IMERG) Final Run (IMERG-Final), against hourly rain gauge observations over Jiangxi province, south central China, in 2019. The main conclusions of this study include but not limited to: (a) considering the precipitation amount, both reanalysis precipitation data and satellite-based precipitation products have similar spatial patterns and show overestimations; (b) IMERG-Final generally outperforms ERA5 and ERA5-Land at multiple temporal scales, especially in terms of CC, FAR and MFI; (c) ERA5 and ERA5-Land precipitation products have similar spatiotemporal error characteristics, and ERA5-Land performs better than ERA5; (d) in the respect of the capabilities of capturing precipitation events, the spatial characteristics of IMERG-Final are the closest to those of rain gauges, while ERA5 and ERA5-Land significantly overestimate the event duration and underestimate the mean event precipitation rate. These findings could help the state-of-the-art model-based and satellite-based precipitation products improve the data quality in the future generations.

1. Introduction

Precipitation estimates with high quality and fine spatiotemporal resolutions play an important role in water resource management, hydrological modeling and climatological analysis (He et al., 2020; Kirschbaum et al., 2016; Sharifi et al., 2019; Ma, Kang, et al., 2018). Ground-based measurements such as rain gauges and weather radars are traditional observation methods to obtain precipitation data at point or regional scales. Nonetheless, due to the uneven spatial distribution of the ground stations and occasional malfunctions, these traditional approaches could not meet the needs of large-scale applications in hydrological, meteorological and climatological communities (Kidd et al., 2016). Precipitation estimates obtained from satellite and reanalysis data could be used for generating spatiotemporal continuous precipitation products, especially in some regions where ground stations are very sparse (e.g., the Tibetan plateau).

With the rapid development of remote sensing techniques and precipitation retrieval algorithms over the past few decades, a series of cost-effective satellite-based precipitation products have been generated. For example, Tropical Rainfall Measuring Mission (TRMM) Multisatellite Precipitation Analysis (TMPA, Kummerow et al, 1998; Huffman et al., 2007), Integrated Multi-satellitE Retrievals for Global Precipitation Measurement (IMERG, Huffman et al, 2019), Climate Hazards Group InfraRed Precipitation with Stations (CHIRPS, Funk et al, 2015), the Climate Prediction Center (CPC) MORPHing technique (CMORPH, Joyce et al, 2004), and Precipitation Estimation from Remotely Sensed Information using Artificial Networks (Ashouri et al., 2014; Hong et al., 2004; PERSIANN, Hsu et al, 1997; Sadeghi et al., 2019). These satellite-based quantitative precipitation estimates make it possible to monitoring the precipitation continuously at a global scale with the increasingly high qualities and resolutions (Kidd & Huffman, 2011; Xu et al., 2019). Additionally, benefiting from a decade of significant progresses in the atmospheric physical models and

numerical assimilation models, several popular atmospheric reanalysis products at a global scale have been released for public, such as ERA-Interim from the European Center for Medium Range Weather Forecasts ((ECMWF) (Dee et al., 2011), MERRA-2 reanalysis from NASA Global Modeling and Assimilation Office (GMAO) (Gelaro et al., 2017), JRA-55 from Japan Meteorological Agency (JMA), and CFSER (version 2) from National Centers for Environmental Prediction (NCEP) (Saha et al., 2014). Recently, ERA5 and ERA5-Land are released by the Copernicus Climate Change Service (C3S), and these two new reanalysis datasets have higher data quality and finer spatiotemporal resolutions compared with their widely used successor, ERA-Interim (Copernicus Climate Change Service (C3S), 2018, 2019; Hersbach et al., 2020).

With increasingly number of precipitation products available across the world, the study of the error characteristics of precipitation products has been paid more and more attention. With the backdrop of global climate change, a detailed investigation of the performance of the multi-source precipitation products will help not only to figure out the error characteristics of reanalysis and satellite-based precipitation products, but also in providing the recommendations of these products to hydrological and meteorological communities according to the different applications (Ma, Xu, et al., 2018; Ma, Zhou, et al., 2018).

Xu et al. (2019) analyzed the similarities and differences between GPM IMERG and Chinese Fengyun 2E and 2G precipitation products against rain gauge data over the mainland China in Summer, 2018. They found that the performances of IMERG are relatively poor at hourly and daily scales. Yu et al. (2020) evaluated CHIRPS, IMERG, and PERSIANN-CCS at daily scale from 2015 to 2018 in terms of various validation metrics over different regions of China. Sui et al. (2020) demonstrated the systematic errors brought by the passive microwave sources of IMERG precipitation data from different sensors, and examined the influences of topography and surface type on these errors. Lu et al. (2020) evaluated the accuracy of IMERG in 2017 over the Yunnan-Kweichow Plateau, and the results that IMERG could capture precipitation events at large scale, but it showed significant overestimations.

Although there are a large number of evaluation studies on satellite-based precipitation products, few investigations have been conducted to assess the quality of the reanalysis precipitation products from ERA5 and ERA5-Land, especially at the hourly scale (Tang et al., 2020). Therefore, in this study, we aim to figure out the error characteristics of ERA5 and ERA5-Land precipitation products as well as IMERG-Final satellite-based precipitation estimates at multiple scales over Jiangxi province in 2019. Meanwhile, the advantages, disadvantages and the error sources of the three precipitation products will be analyzed and discussed.

2. Study Area

Jiangxi province is one of the most densely populated and agriculturally productive provinces in China, with the longitude and latitude range between 113°34′36″–118°28′58″E and 24°29′14″–30°04′41″N, covering an area of 166,900 km^2 (Figure 1). Jiangxi province is located on the south bank of the middle and lower reaches of the Yangtze River in the south-central part of mainland China, and is dominated by a subtropical humid monsoon climate with obvious seasonal differences (Xie et al., 2013). The average annual temperature of the region varies from 16.3°C to 19.5°C and generally increases from north to south. Jiangxi province is one of the rainy areas in China. The annual precipitation is 1,340 mm–1,945 mm, while the uneven temporal distribution of which at seasonal and yearly scales results in the frequent occurrences of droughts and floods in Jiangxi province (Xu et al., 2014; Zhang et al., 2016). The spatial distribution of the digital elevation model (DEM) and rain gauge network in Jiangxi province is shown in Figure 1. The terrain of Jiangxi province is relatively high in the south and low in the north, which is conductive to the convergence of the water resources. According to the official statistics, there are more than 2,400 rivers in the province with a total length of 18,400 km. Covered with dense rivers and lakes, Jiangxi province has abundant surface water resources and relatively developed hydrographic nets, which promotes the biodiversity in the province and plays an important role in shipping and irrigation.
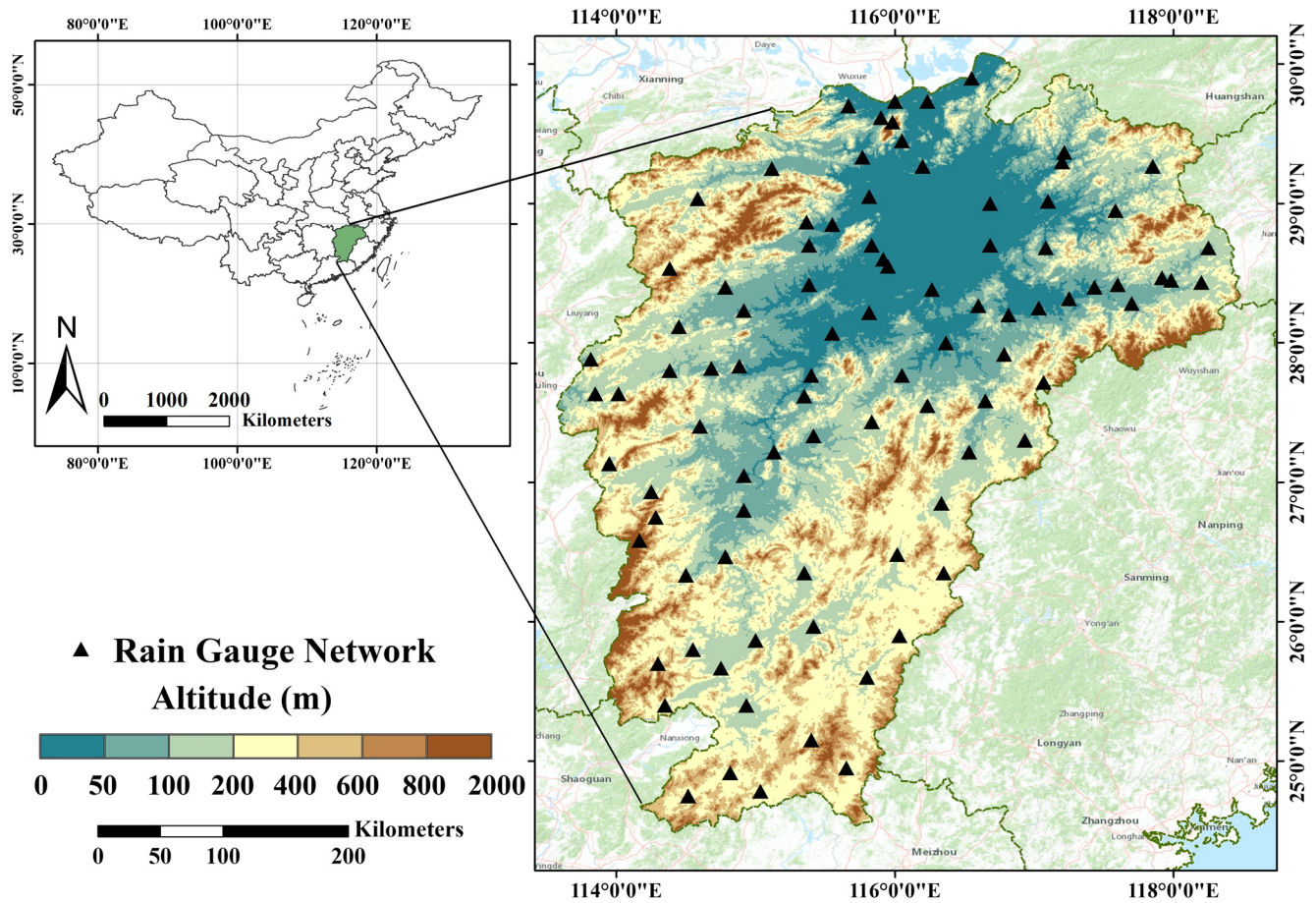
Figure 1. Spatial distributions of the Digital Elevation Model (DEM) and rain gauge network in Jiangxi province.

3. Data and Method

3.1. ERA5

The fifth-generation global atmospheric analysis data set of the European Center for Medium-Range Weather Forecasts (ECMWF) (ERA5, 0.25°, hourly, global) has considerably finer spatiotemporal resolutions and temporal coverage compared with its widely used predecessor, ERA-Interim (Dee et al., 2011; Hersbach et al., 2020), thus allowing its further application in climatological, hydrological and meteorological communities. In this study, we use the variable of total precipitation in ERA5, which represents the accumulation of liquid and solid precipitation that falls to the land surface. ERA5 total precipitation products can be downloaded from the website https://doi.org/10.24381/cds.adbb2d47. The detail information of the precipitation products used in this study is listed in Table 1.

Table 1
Summary of Reanalysis and Satellite-Based Precipitation Datasets Used in This Study

Data set	Full name of the data set	Resolution	Period	Reference
ERA5	European Center for Medium-Range Weather Forecasts Reanalysis-5	0.25°/1.0 h	1950–present	Copernicus Climate Change Service (C3S), 2018
ERA5-Land	European Center for Medium-Range Weather Forecasts Reanalysis-5-Land	0.10°/1.0 h	1979–present	Copernicus Climate Change Service (C3S), 2019
IMERG-Final	Integrated Multi-satellitE Retrievals for Global Precipitation Measurement	0.10°/0.5 h	2000–present	Huffman et al., 2019

3.2. ERA5-Land

The ERA5-Land reanalysis data set (0.1°, hourly, global land regions) covers the period from 1981 to present, and is a new generation of global (land) reanalysis of ECMWF. ERA5-Land is opened to the public after the recent release of ERA5 climate reanalysis from 1979 onwards (Copernicus Climate Change Service (C3S), 2018, 2019; Hersbach et al., 2020). ERA5-Land provides much more information at finer spatiotemporal resolutions than ERA5, and in some way could be the first hourly data set that describes the water and energy cycles at the grid spacing of 0.1° on global land surface for nearly three decades. Same as ERA5 precipitation products, the variable of total precipitation in ERA5-Land is used. The ERA5-Land reanalysis data set can be downloaded from https://doi.org/10.24381/cds.e2161bac.

3.3. IMERG-Final

Integrated Multi-satellitE Retrievals for Global Precipitation Measurement (IMERG) is the primary gridded precipitation product provided by NASA, which intends to intercalibrate, merge and interpolate a suite of microwave-based precipitation estimates from the GPM constellation of research and operational satellites, microwave-calibrated infrared-based observations and gauge-based measurements to comprehensively understand the physics and spatiotemporal variability of precipitation across the Earth (Huffman et al., 2019). IMERG Final Run V06B (0.1°, half-hourly), the version we used in this study, is a research-quality gridded global precipitation product calibrated by GPCC monthly monitoring product and can be downloaded from https://gpm.nasa.gov/data/directory. The hourly IMERG-Final precipitation data is obtained by averaging the two corresponding half-hourly data in the specific hour.

3.4. Rain Gauge Data

The hourly point-based precipitation datasets from 91 automatic rain gauge stations over Jiangxi province in 2019 are collected from the National Meteorological Information Center (NMIC) of China Meteorological Administration (CMA). The spatial distribution of rain gauge network in Jiangxi province is shown in Figure 1. Meanwhile, the rain gauge precipitation datasets are quality controlled with the accuracy close to 100%. Hourly rain gauge data can be downloaded from http://data.cma.cn. Daily, monthly and yearly point-based precipitation datasets are obtained by accumulating the hourly data in the specific temporal ranges.

3.5. Validation Metrics

In this study, seven validation metrics including correlation coefficient (CC), Relative bias (bias), Root mean square error (RMSE), Probability of detection (POD), False alarm ratio (FAR), Critical success index (CSI) and Multi-source fusion index (MFI) are used to comprehensively evaluate ERA5, ERA5-Land and IMERG-Final at multiple scales. CC generally depicts the agreements between precipitation products and ground observations, with values range from 0 to 1. bias and RMSE are widely used to quantitatively describe the degree of deviation between precipitation products and ground observations. POD, FAR and CSI represent the precipitation products' capability of capturing the precipitation events correctly. MFI is a index that comprehensively taking into account the performances of precipitation products in terms of statistical indices and contingency indices, and the larger value of MFI means the better performance of precipitation products. In addition, the thresholds of 0.1 mm hour-1 for hourly precipitation events and 1 mm day-1 for daily events are used to discriminate the rain and no-rain events. The formula and perfect value of those validation metrics are shown in Table 2.

4. Results

4.1. Spatial Distributions in Terms of Precipitation Amount

The spatial patterns of accumulated annual precipitation of point-based rain gauges, spatial-continuous rain gauge measurements based on inverse distance weighted (IDW), ERA5, ERA5-Land and IMERG-Final over Jiangxi province in 2019 are displayed in Figures 2a–2e, respectively. As shown in Figures 2a and 2b, the annual precipitation amount in central Jiangxi is relatively large (>1,800 mm/year), followed by the

Table 2
List of the Validation Metrics for Evaluating Reanalysis and Satellite-Based Precipitation Products in the Study

Name	Formula	Perfect value
Correlation coefficient (CC)	$CC = \sqrt{\dfrac{\sum_{i=1}^{n}\left(O_i - \overline{O}\right)^2 \left(P_i - \overline{P}\right)^2}{\sum_{i=1}^{n}\left(O_i - \overline{O}\right)^2 \times \sum_{i=1}^{n}\left(P_i - \overline{P}\right)^2}}$	1
Relative bias (bias)	$bias = \dfrac{\sum_{i=1}^{n}\left(P_i - O_i\right)}{\sum_{i=1}^{n} O_i} \times 100\%$	0
Root mean square error (RMSE)	$RMSE = \sqrt{\dfrac{1}{n}\sum_{i=1}^{n}\left(P_i - O_i\right)^2}$	0
Probability of detection (POD)	$POD = \dfrac{H}{H + M}$	1
False alarm ratio (FAR)	$FAR = \dfrac{F}{H + F}$	0
Critical success index (CSI)	$CSI = \dfrac{H}{H + M + F}$	1
Multi-source fusion index (MFI)	$MFI = 1 - \sqrt{\left(CC - 1\right)^2 + bias^2 + \left(CSI - 1\right)^2}$	1

Note. O_i, the amount of precipitation observed by real data; $\overline{O}$, the average true values, P_i, the estimated values of the precipitation product; $\overline{P}$, the average estimated precipitation; n, the number of precipitation pairs of real data and the corresponding product estimates; H, observed precipitation event correctly detected by product estimates; M, observed precipitation event not detected by product estimates; F, precipitation event detected by product estimates but not observed.

southern part (<1,800 mm/year), and the northern region has the lowest precipitation amount (<1,600 mm/year). ERA5 and ERA5-Land share the similar spatial patterns of total precipitation, while the latter has a finer spatial resolution and hence shows more spatial details than ERA5. Compared with rain gauge observations, ERA5 and ERA5-Land overestimate precipitation in the northeastern and southern parts, and IMERG-Final significantly overestimates precipitation, especially in the central regions of Jiangxi province.

4.2. Numerical Distributions of the Validation Metrics

The general daily comparisons among ERA5, ERA5-Land and IMERG-Final against rain gauge observations over Jiangxi province in 2019, are demonstrated in Figure 3. Generally, IMERG-Final outperforms ERA5 and EAR5-Land at daily scale as far as CC and RMSE are concerned. It is obvious that the CC value of IMERG-Final (~0.74) are the largest among the values of three precipitation products, which means that IMERG-Final shows best agreement with ground observations. ERA5-Land outperforms ERA5 at daily scale, with CC values around 0.64 and 0.62, respectively. The validation results revealed by RMSE are similar with those represented by CC. In terms of bias, the deviations of ERA5 and ERA5-Land are close to zero, while IMERG-Final shows small degree of overestimation (bias~8.96%). In addition, most of the points are distributed near the origin, which indicates that the intensities of precipitation amount at meteorological scale are heavily skewed toward zero.

Figure 4 illustrates the numerical distribution of validation indicators for ERA5, ERA5-Land and IMERG-Final in terms of CC, bias, RMSE, POD, FAR, and MFI against ground truth at hourly scale over Jiangxi province in 2019. And the mean values of validation metrics for the three precipitation products at hourly scale are shown in Table 3. As for the statistical metrics, the distribution of CC values shows the biggest difference for ERA5, ERA5-Land and IMERG-Final, with the mean values around 0.26, 0.27 and 0.48, respectively. Bias values of the three precipitation products have similar distribution, and the index
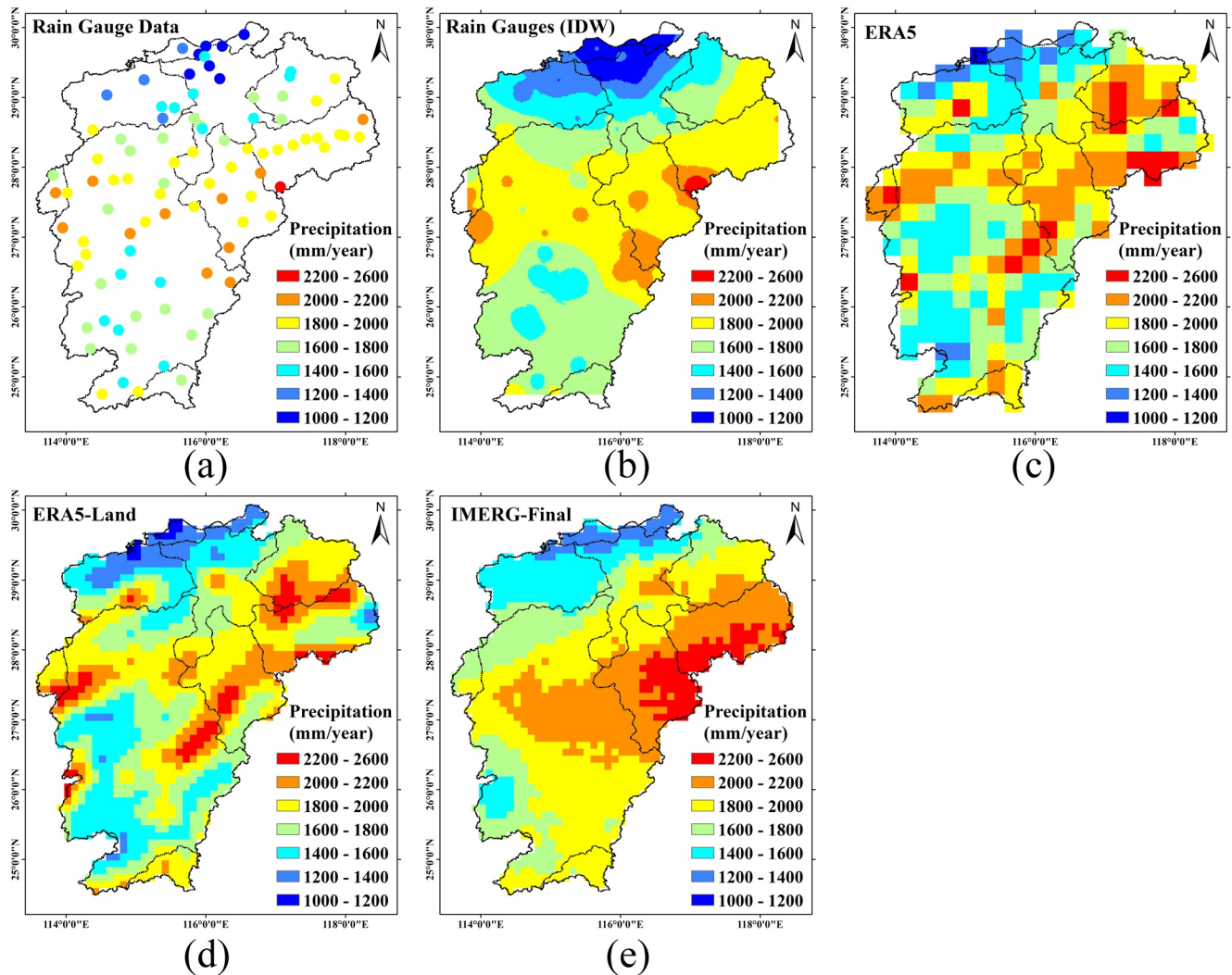
Figure 2. The spatial patterns of annual total precipitation estimated by (a) point-based rain gauges, (b) spatial-continuous rain gauge measurements based on inverse distance weighted (IDW), (c) ERA5, (d) ERA5-Land and (e) IMERG-Final over Jiangxi province in 2019.

value corresponding to the lower bound of IMERG-Final (∼−20%) is larger than those of ERA5 and ERA5-Land (∼−30%), which means that the underestimation degree of IMERG-Final is slighter than the other two products. The mean POD values of ERA5 and ETA5-Land (∼0.74 and 0.74) are overall larger than that of IMERG-Final (∼0.60), indicating that the false negative proportion in real precipitation events of ERA5 and ERA5-Land are smaller than that of IMERG-Final. Nonetheless, the numerical distribution of FAR shows a contrary result. The false positive proportion in estimated precipitation events of IMERG-Final is smaller than those in ERA5 and ERA5-Land. Regarding MFI, IMERG-Final performs significantly better than ERA5 and ERA5-Land, with the mean value around 0.04, 0.05, and 0.19, respectively.

4.3. Temporal Distributions of the Validation Metrics

The temporal patterns of the validation metrics at specific hourly scale for ERA5, ERA5-Land and IMERG-Final compared to the ground measurements are displayed in Figure 5. It is notable that there is a significant difference in the temporal patterns of CC values between satellite-based and reanalysis precipitation products, and IMERG-Final generally performs better than ERA5 and ERA5-Land. Generally, both the performances of reanalysis and satellite-based precipitation products are poorer at 03:00 (meant 03:00 in Coordinated Universal Time, which is the same as below) and 16:00 than other periods in 1 day. With regard
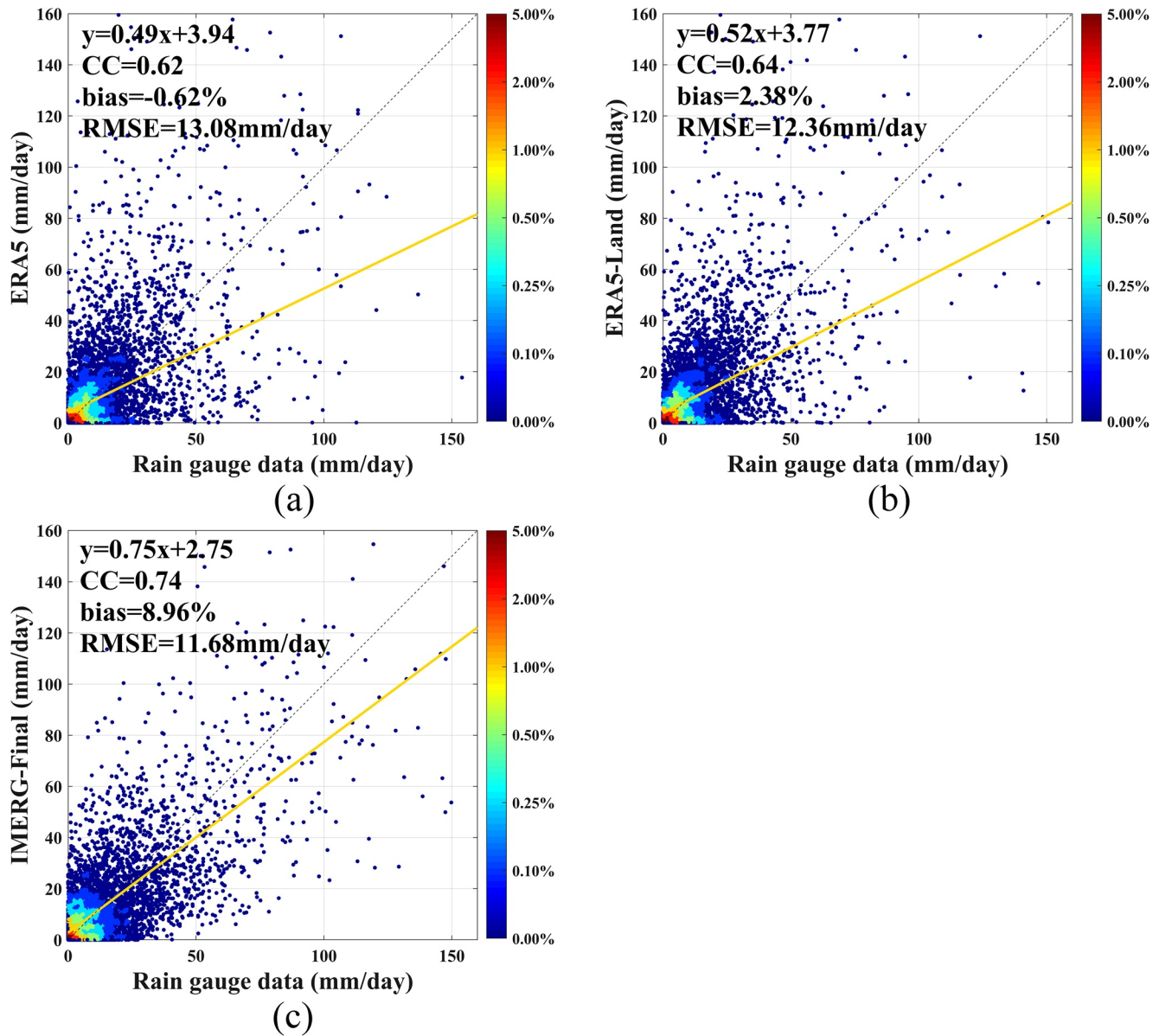
Figure 3. Scatterplots of evaluations on (a) ERA5, (b) ERA5-Land and (c) IMERG-Final at daily scale over Jiangxi province in 2019.

to RMSE, the temporal patterns of three products are very similar, with the peak value reaches at 08:00. As for POD, IMERG-Final have lower values in almost every specific hour in one day, and the period when the peak values of the three products reach are the same as that of RMSE. The FAR values of IMERG-Final are smaller than those of ERA5 and ERA5-Land before 10:00, and are significantly larger than those of reanalysis precipitation products from 11:00 to 23:00. The similar phenomenon could also be found in Figure 5g, except for the period from 17:00 to 18:00 and from 21:00 to 23:00.

Figure 6 shows temporal patterns of performances on ERA5, ERA5-Land and IMERG-Final against rain gauge observations at monthly scale. The temporal patterns of ERA5 and ERA5-Land are very similar in terms of almost all metrics. The CC of ERA5 and ERA5-Land reaches its highest value in March (~0.35), and is smaller than 0.25 in the remaining months, especially in August and September (~0.13). Similarly, the CC value of IMERG-Final is also the largest in March, and the performance from March to June is better than other months in 2019. The values of bias are relatively high in wet season and low in dry season, and the most obvious difference between reanalysis data and satellite-based data is that IMERG shows a peak in
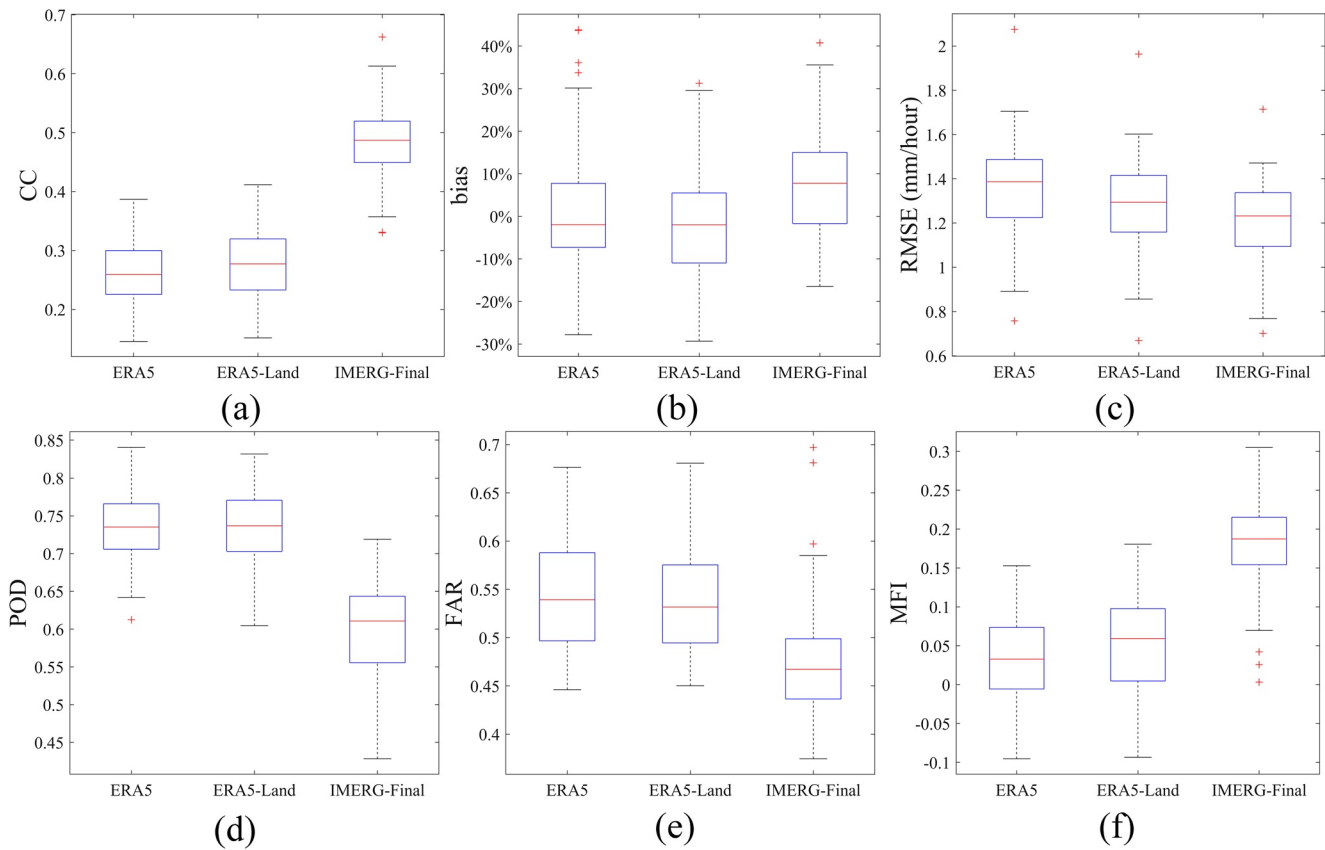
Figure 4. The numerical distributions of validation metrics for ERA5, ERA5-Land and IMERG-Final at hourly scale in terms of (a) correlation coefficient (CC), (b) Relative bias (bias), (c) Root mean square error (RMSE), (d) Probability of detection (POD), (e) False alarm ratio (FAR) and (f) Multi-source fusion index (MFI).

August (~151%), while the peaks of ERA5 and ERA5-Land are in June (~135% and 138%, respectively). In November, bias values of the reanalysis precipitation data are close to zero, while IMERG-Final presents a relatively high value of bias (~68.4%). The RMSE of each product reaches the maximum in July. As for contingency metrics such as POD, the performances of reanalysis data are significantly better than that of satellite-based data. Generally, all products perform better in the first half of the year in terms of POD. The POD values of ERA5 and ERA5-Land are around 0.6 from February to July, and the POD values of IMERG-Final are around 0.5 from March to September. The FAR value of each product is smaller in January–March, and larger in August, compared with the other months in 2019. In terms of MFI, each product performs better from January to March, but not performs well from August to October.

4.4. Spatial Distributions in Terms of Precipitation Events

Figure 7 demonstrates the spatial distributions of performances in terms of POD, FAR and MFI estimated by ERA5, ERA5-Land and IMERG-Final at hourly scale over Jiangxi province in 2019. The POD values of IMERG are mostly distributed between 0.40 and 0.65, with the high values in northern parts of Jiangxi province. Additionally, the differences of spatial patterns between ERA5 and ERA5-Land are not significant. The FAR index of ERA5 and ERA5-Land performs better in the northern regions than in the southern regions, and the POD index performs better in the northeast than the other parts of Jiangxi province. As far as MFI is concerned, the three products in the north of Jiangxi province generally
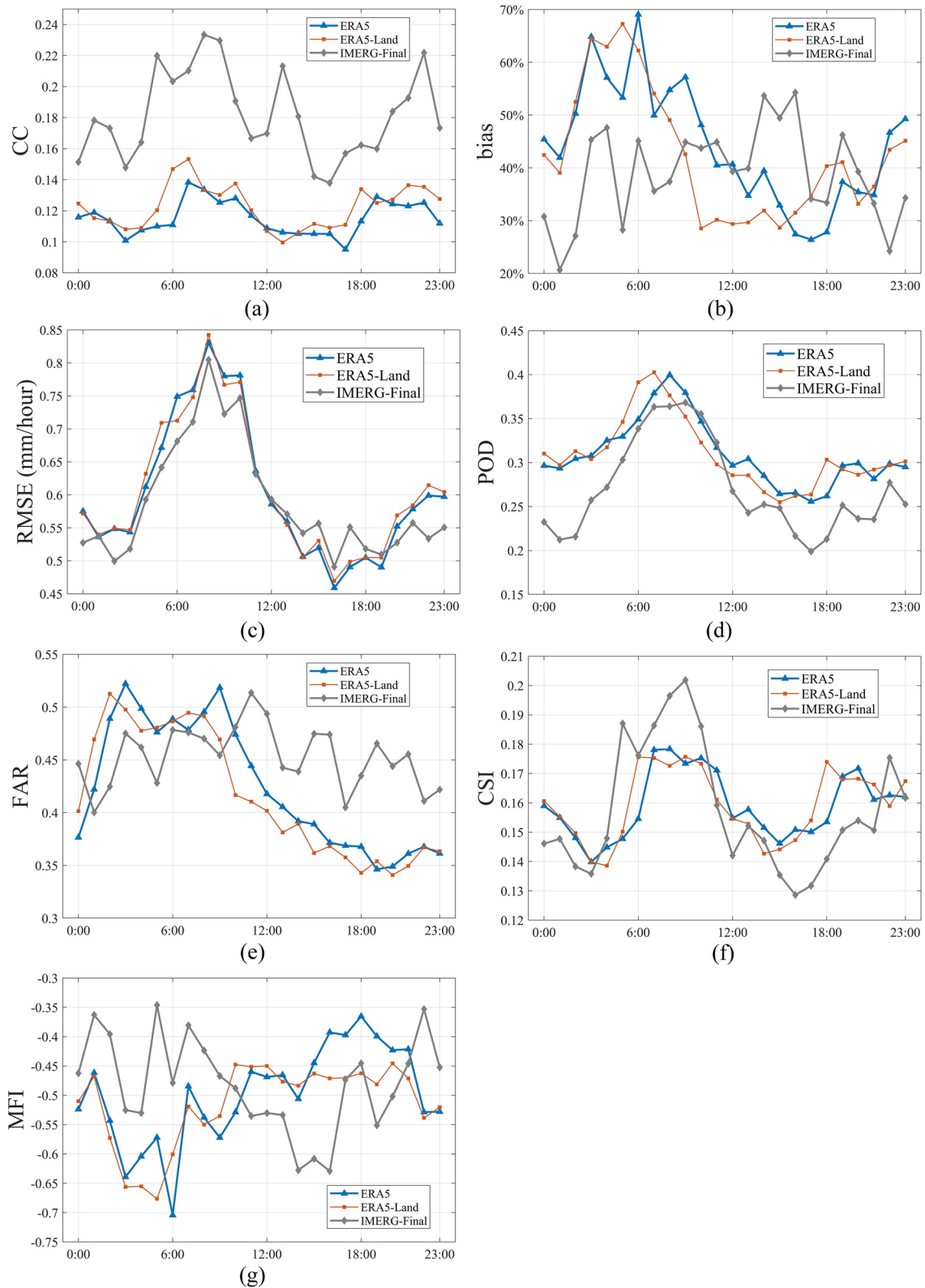
Table 3
Summaries of the Results for ERA5, ERA5-Land and IMERG-Final, at Hourly Scale Over Jiangxi Province in 2019

Index	ERA5	ERA5-land	IMERG-final
CC	0.26	0.27	0.48
bias (%)	−0.92	−2.54	6.24
RMSE (mm/hour)	1.37	1.29	1.22
POD	0.74	0.74	0.60
FAR	0.54	0.54	0.48
CSI	0.39	0.39	0.38
MFI	0.04	0.05	0.19

Figure 5. Temporal patterns of performances on ERA5, ERA5-Land and IMERG-Final in terms of (a) correlation coefficient (CC), (b) Relative bias (bias), (c) Root mean square error (RMSE), (d) Probability of detection (POD), (e) False alarm ratio (FAR), (f) Critical success index (CSI) and (g) Multi-source fusion index (MFI) against rain gauge observations at specific hourly scale, respectively.
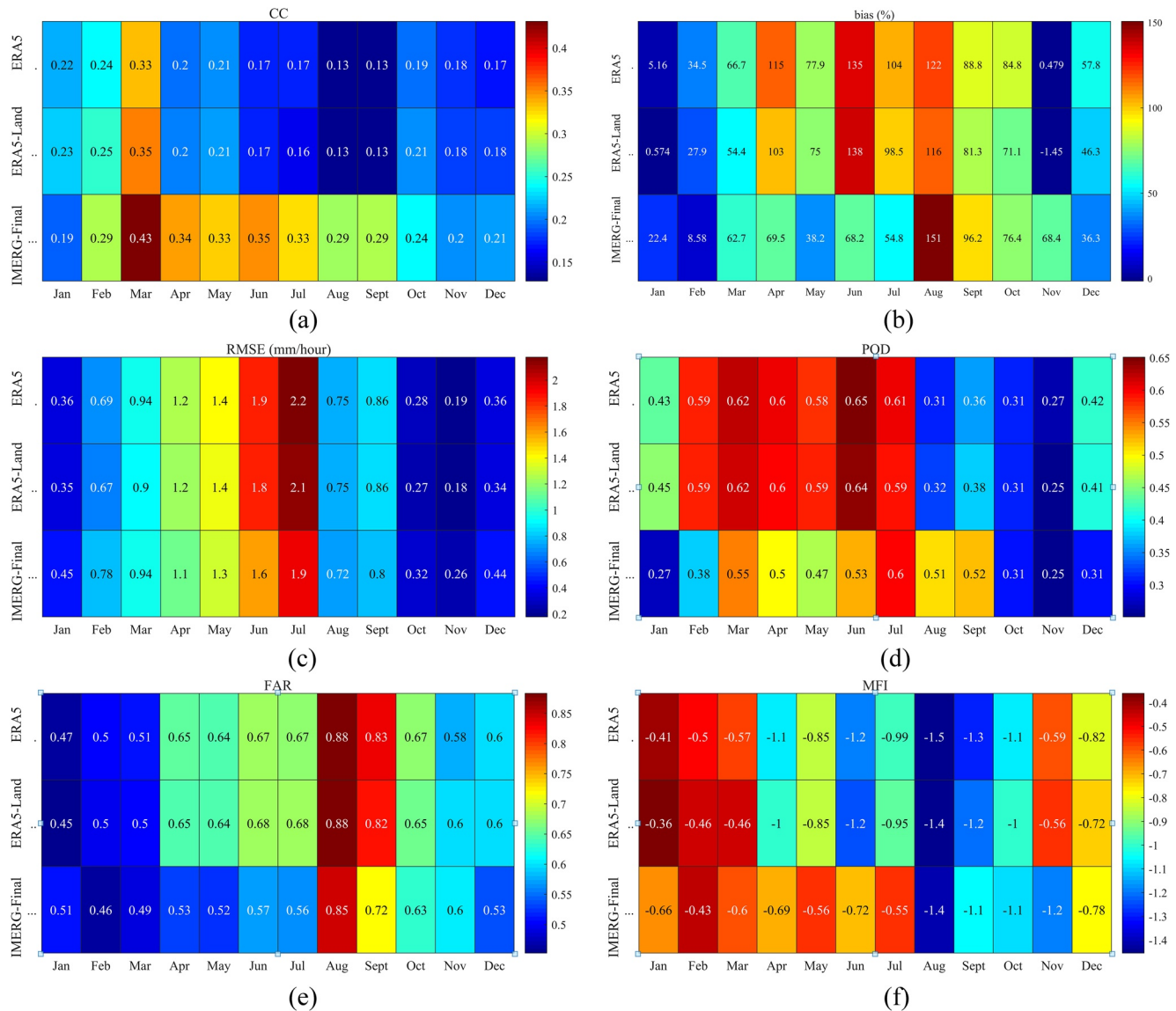
Figure 6. Temporal patterns of performances on ERA5, ERA5-Land and IMERG-Final in terms of (a) correlation coefficient (CC), (b) Relative bias (bias), (c) Root mean square error (RMSE), (d) Probability of detection (POD), (e) False alarm ratio (FAR) and (f) Multi-source fusion index (MFI) against rain gauge observations at monthly scale, respectively.

outperform than those in the south. The MFI values of IMERG-Final are mostly between 0.15 and 0.35, and the values of ERA5 and ERA5-Land are mostly distributed between −0.1 and 0.15.

Figure 8 presents the spatial patterns of characteristics in terms of the metrics of precipitation events, such as number of events, event duration and mean event precipitation rate, captured by rain gauges, ERA5 ERA5-Land and IMERG-Final at hourly scale over Jiangxi province in 2019. In this study, a complete precipitation event is composed of continuous precipitation data, and all precipitation events happened over Jiangxi province in 2019 are selected to calculate the metrics. Event duration means the temporal duration of the precipitation event. And mean event precipitation rate presents the mean precipitation rate (mm/hour) of the specific precipitation event. Considering the event duration and mean event precipitation rate, IMERG-Final presents the closest patterns among the three precipitation products compared with the information of precipitation events captured by the rain gauge data. However, as for the number of events captured by the three precipitation products, IMERG-Final shows a significant overestimation in the northern parts of Jiangxi province and an underestimation in the eastern regions. The reanalysis datasets have
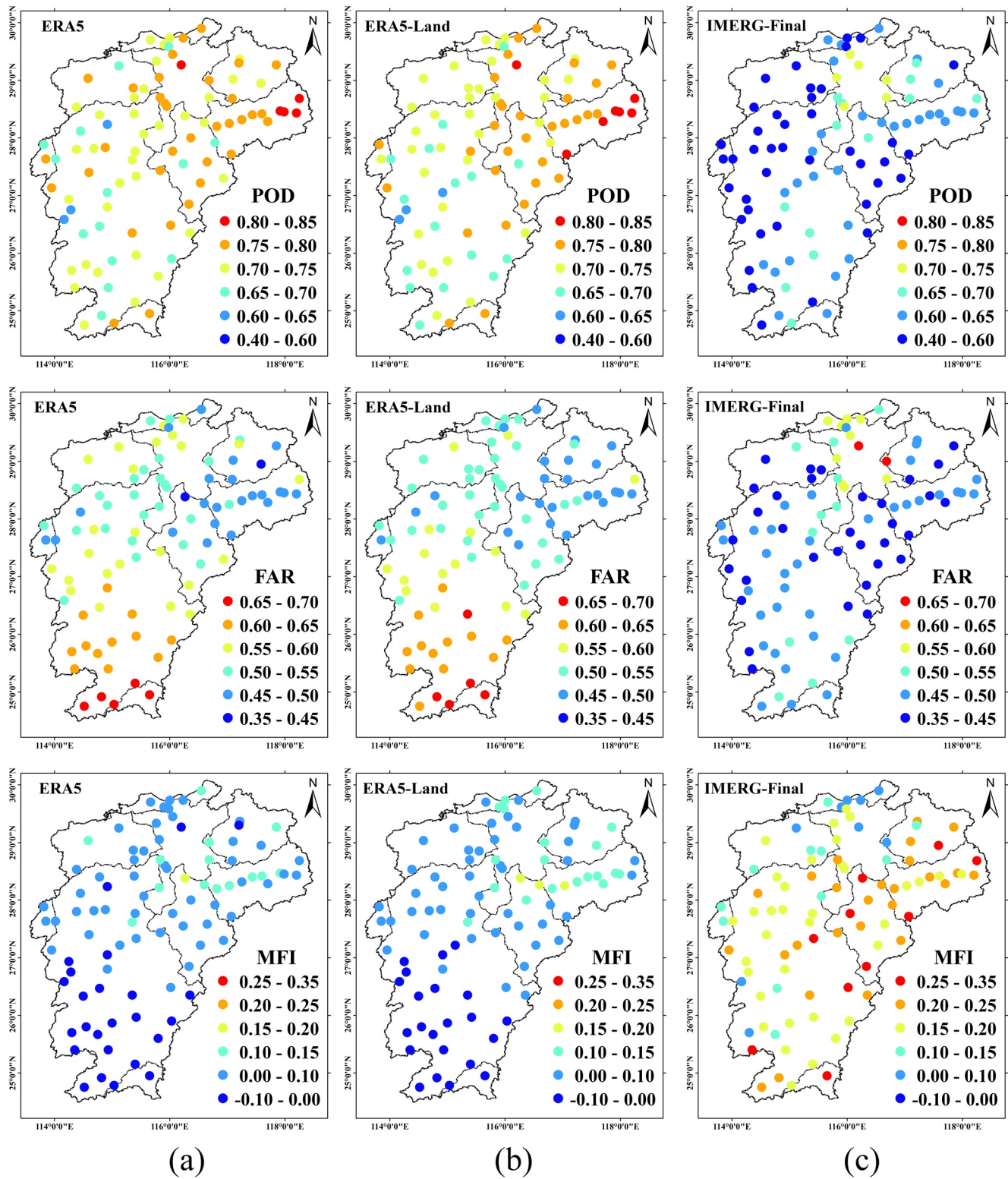
Figure 7. Spatial distributions of performances in terms of Probability of detection (POD), False alarm ratio (FAR) and Multi-source fusion index (MFI) estimated by (a) ERA5, (b) ERA5-Land and (c) IMERG-Final at hourly scale over Jiangxi province in 2019.
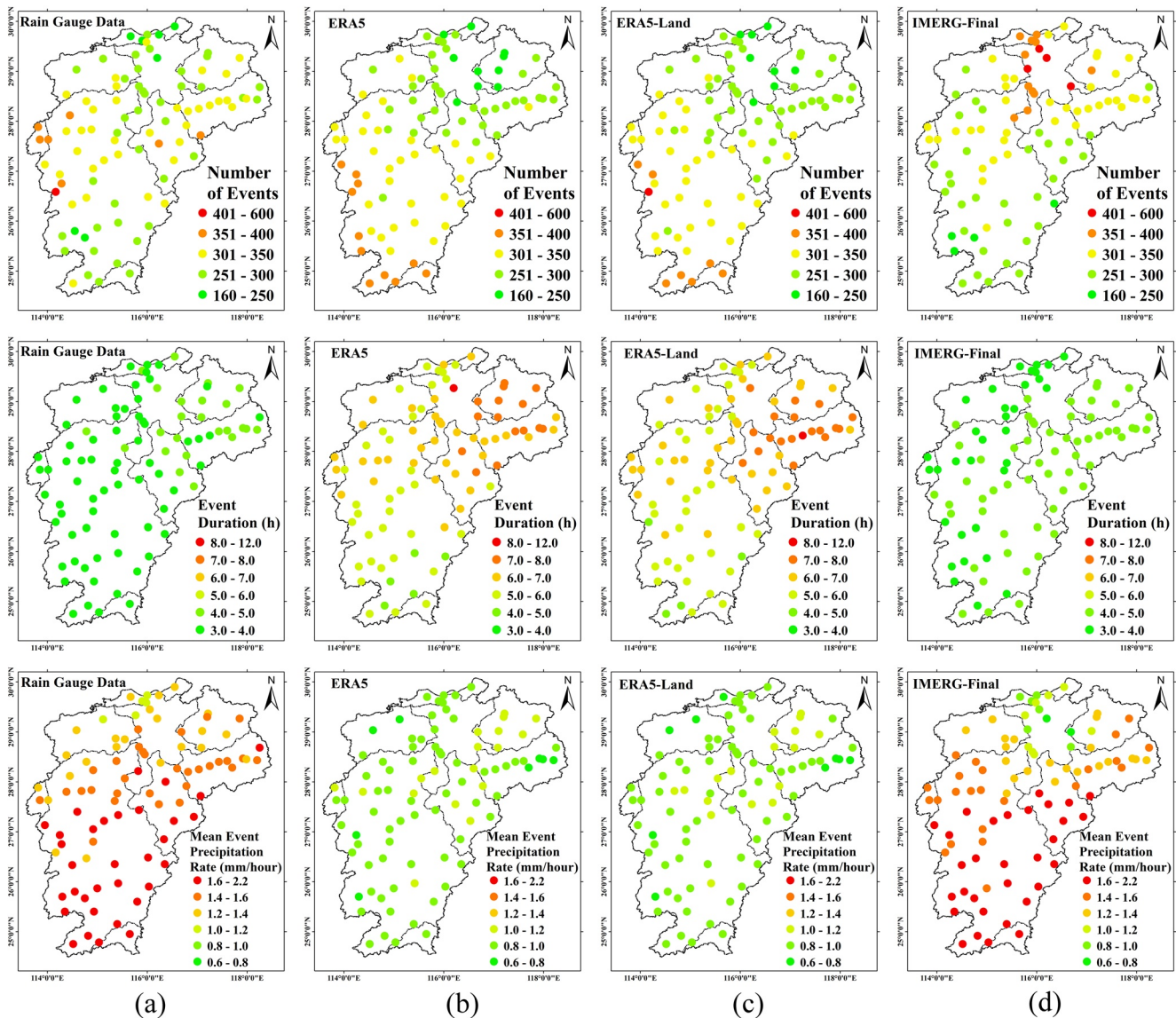
Figure 8. Spatial patterns of characteristics in terms of precipitation events captured by (a) rain gauges, (b) ERA5, (c) ERA5-Land and (d) IMERG-Final at hourly scale over Jiangxi province in 2019.

similar spatial patterns, but show significant overestimations in precipitation event duration and underestimations in mean event precipitation rate. As for the number of events, ERA5 and ERA5-Land perform better than IMERG-Final in the north and east regions of Jiangxi province, while overestimate the numbers in southern parts.

5. Discussion

5.1. Advantages and Disadvantages of the Three Precipitation Products

IMERG-Final, ERA5, ERA5-Land have their advantages and disadvantages across the study area, in terms of data accuracy, data release latency, spatiotemporal resolution and space-time coverage. The three precipitation products share the same temporal resolution of 1 h, while IMERG-Final and ERA5-Land have finer spatial resolution at the grid spacing of 0.1°, compared with the 0.25° spatial resolution of ERA5. Considering the data accuracy, IMERG-Final is more suitable for practical applications in hydrological and meteorological fields than ERA5 and ERA5-Land in Jiangxi province. What's more, IMERG-Final has a

quasi-global spatial coverage, which is the same as ERA5 precipitation product. In contrast, the spatial coverage of ERA5-Land is confined to the global land area with considerable missing data at the junction of land and sea. Therefore, ERA5-Land precipitation product could not be used for the applications related to the ocean area, for instance, researches about quantifying the global water cycle. In the respect of data release latency, ERA5 significantly outperforms than ERA5-Land and IMERG-Final. The update frequency of ERA5 reanalysis precipitation data is about 1 day, while ERA5-Land data is released monthly with a delay of about 3 months relatively to actual date, and IMERG-Final has the latency of about 3.5 months. Benefiting from the short data release latency, ERA5 precipitation product has the potential to be used in the near-real-time hydrological and meteorological applications (Mastrantonas et al., 2019; Massari et al., 2019; Wang et al., 2019; Xu et al., 2019). As for the temporal coverage, the reanalysis precipitation products do have superiorities. Even though IMERG-Final has been retrospected to the TRMM era (2000 to present) at the end of September 2019, the time span of IMERG-Final is relatively short compared with those of ERA5 and ERA5-Land. The temporal coverage of ERA5-Land and ERA5 precipitation data is from 1981 to present and from 1950 to present, respectively, and the back extension of ERA5-Land (1950–1980) is planned for public release in early 2021 (Copernicus Climate Change Service (C3S), 2018, 2019; Hersbach et al., 2020).

5.2. Error Source Analysis of the Three Precipitation Products

The spatial inconsistency between the point-based rain gauge data and satellite-based or reanalysis precipitation data could have potential effects on the error characteristics revealed by the evaluation results (Tang et al., 2018). For instance, the center coordinates of the grids are different in IMERG-Final and ERA5 (or ERA5-Land) precipitation products, which are deviated by 0.05°. This phenomenon may lead to the different error characteristics in evaluating the reanalysis and satellite-based datasets. ERA5 and ERA5-Land generally represent non-zero, as pointed by Hersbach et al. (2020), which could explain the phenomenon that the POD values as well as the FAR values of ERA5 and ERA5-Land are relatively high. ERA5-Land has similar error characteristics with ERA5, and the performances of the former are slightly better than the latter. This might be explained by the fact that ERA5-Land is downscaled from ERA5 with thermo-dynamical orographic adjustment driven by near surface variables, such as temperature.

There are many studies on the error analysis of IMERG precipitation data. For example, Zhu et al. (2020) tried to reveal the potential connections between geographical features and the error patterns of IMERG precipitation product, and found that geographical features had strong relationships with the validation metrics of IMERG. Related studies like that could provide valuable references for the improvement of the precipitation quality in the next generation. Although IMERG-Final performs better than ERA5 and ERA5-Land, users still pay great attention to the not so satisfying performance of IMERG at hourly and diurnal scales. Therefore, some algorithms and methods, such as downscaling, gauge-based calibration and retrospective studies, could be applied to yield the long-term precipitation products with higher qualities and finer spatiotemporal resolutions (Ma, He, et al., 2019; Ma, Xu, et al., 2019). Explorations have been made by some researchers. Take the study presented by Ma et al. (2017) for example, they introduced an algorithm to downscale the TRMM Multi-satellite Precipitation Analysis (TMPA) 3B43 Version 7 data set to a 1 km spatial resolution over the Qinghai–Tibet Plateau. Taking the spatial scale effects between precipitation and environmental variables into account, downscales performed significantly better than other common algorithms and the original TMPA data. Moreover, the algorithm removed the systematic anomalies in the original TMPA data. The contribution of study is significant to downscaling-related researches. By way of illustration, Ma et al. (2020) proposed a new calibration algorithm, namely daily spatio-temporal disaggregation calibration algorithm (DSTDCA), to remove the systematic bias and random errors in GPM IMERG (0.1° and half-hourly) using ground measurements, Asian precipitation–highly resolved observational data integration toward evaluation of water resources (APHRODITE, 0.25° and daily). And a new data set called AIMERG for Asian area were produced, with better performances than IMERG at multiple scales in terms of statistical metrics and in specific precipitation events. Such study made a breakthrough in the algorithm exploration for improving the quality of the state-of-the-art precipitation products with fine spatiotemporal resolutions. Nevertheless, researches about the error characteristics and quality improvement of reanalysis data, especially ERA5 and ERA5-Land, are relatively scarce, which have great potentials in the future study.

6. Conclusion

Reanalysis and satellite-based precipitation products with fine spatiotemporal resolution are two primary sources of precipitation estimates for large-scale applications in climatological, hydrological and meteorological communities. In this study, three recently released gridded precipitation products, namely ERA5, ERA5-Land and IMERG-Final, are evaluated against rain gauge observations to figure out their error characteristics over Jiangxi province, China, in 2019. The main conclusions of this study are as follows:

1. both reanalysis precipitation data and satellite-based precipitation products have similar spatial patterns and show overestimations, considering the accumulated annual precipitation amount;
2. generally, except for the performance revealed by POD, IMERG-Final outperforms ERA5 and ERA5-Land over Jiangxi province at multiple temporal scales, especially in terms of CC, FAR and MFI;
3. ERA5 and ERA5-Land precipitation products have similar error characteristics, and the latter, which has finer spatial resolution, performs better than ERA5;
4. according to the validation results of the capabilities of capturing precipitation events, the spatial characteristics of IMERG-Final are the closest to those of rain gauges among the three products, while ERA5 and ERA5-Land significantly overestimate the event duration and underestimate the mean event precipitation rate.

The comprehensive evaluation of the performance of the state-of-the-art reanalysis and satellite-based precipitation products at multiple spatiotemporal scales could provide not only the error characteristics of the current precipitation products with relatively high quality and fine resolution, but also the valuable references for improving the retrieval algorithms in the next generation. Additionally, for further exploration of the error characteristics of reanalysis and satellite-based precipitation products, hydrological models such as CREST could be used to evaluate the performances of precipitation products against observed streamflow records (Wang et al., 2011).

Data Availability Statement

Hourly precipitation data from the fifth generation ECMWF reanalysis is available from https://doi.org/10.24381/cds.adbb2d47 (ERA5, Copernicus Climate Change Service (C3S), 2018). Hourly precipitation data from the fifth generation ECMWF reanalysis (Land) is available from https://doi.org/10.24381/cds.e2161bac (ERA5-Land, Copernicus Climate Change Service (C3S), 2019). Hourly precipitation data from Integrated Multi-satellitE Retrievals for Global Precipitation Measurement is available from https://arthur-houhttps.pps.eosdis.nasa.gov/gpmdata/(IMERG, Huffman et al, 2019). Hourly rain gauge observations are obtained from http://data.cma.cn/.

References

Ashouri, H., Hsu, K., Sorooshian, S., Braithwaite, D. K., Knapp, K. R., Cecil, L. D., et al. (2014). Persiann-cdr: Daily precipitation climate data record from multisatellite observations for hydrological and climate studies. *Bulletin of the American Meteorological Society*, *96*(1), 69–83.

Copernicus Climate Change Service (C3S) (2018). *ERA5: Fifth generation of ECMWF atmospheric reanalysis of the global climate [data set]*, Copernicus climate change Service climate data store (CDS). https://doi.org/10.24381/cds.adbb2d47

Copernicus Climate Change Service (C3S) (2019). *ERA5-Land: Fifth generation of ECMWF atmospheric reanalysis of the global climate [data set]*, Copernicus climate change Service climate data store (CDS). https://doi.org/10.24381/cds.e2161bac

Dee, D. P. R., Uppala, S., Vitart, P., Poli, P., Kobayashi, S., et al. (2011). The era-interim reanalysis: Configuration and performance of the data assimilation system. *Quarterly Journal of the Royal Meteorological Society*, *137*(656), 553–597. https://doi.org/10.1002/qj.828

Funk, C., Peterson, P., Landsfeld, M., Pedreros, D., Verdin, J., Shukla, S., et al. (2015). The climate hazards infrared precipitation with stations—A new environmental record for monitoring extremes. *Scientific Data*, *2*, 150066. https://doi.org/10.1038/sdata.2015.66

Gelaro, R., Mccarty, W., Suárez, M. J., Todling, R., & Zhao, B. (2017). The modern-era retrospective analysis for research and applications, version 2 (merra-2). *Journal of Climate*, *30*(14). https://doi.org/10.1175/jcli-d-16-0758.1

He, X., Pan, M., Wei, Z. W., Wood, E., & Sheffield, J. (2020). A Global Drought and Flood Catalogue from 1950 to 2016. *Bulletin of the American Meteorological Society*. *101*. E508–E535. https://doi.org/10.1175/bams-d-18-0269.1

Hersbach, H., Bell, B., Berrisford, P., Hirahara, S., Horányi, A., Muñoz-Sabater, J., et al. (2020). The ERA5 global reanalysis. *Quarterly Journal of the Royal Meteorological Society*, *146*, 1999–2049. https://doi.org/10.1002/qj.3803

Hong, Y., Hsu, K. L., Sorooshian, S., & Gao, X. (2004). Precipitation estimation from remotely sensed imagery using an artificial neural network cloud classification system. *Journal of Applied Meteorology*, *36*(12), 1176–1190. https://doi.org/10.1175/jam2173.1

Hsu, K., Gao, X., Sorooshian, S., & Gupta, H. (1997). Precipitation estimation from remotely sensed information using artificial neural networks. *Journal of Applied Meteorology*, *36*(9), 1176–1190. https://doi.org/10.1175/1520-0450(1997)036<1176:pefrsi>2.0.co;2

Huffman, G., Bolvin, A., Dan, B., Hsu, K., Joyce, R., & Xie, P. (2019). *NASA Global Precipitation Measurement (GPM) Integrated Multi-satellitE Retrievals for GPM (IMERG). Algorithm theoretical basis document (ATBD) version 06* (p. 38pp). NASA/GSFC.

Huffman, G., Bolvin, D., Nelkin, E., Wolff, D., Adler, R., Gu, G., et al. (2007). The TRMM Multisatellite Precipitation Analysis (TMPA): Quasi-global, multiyear, combined-sensor precipitation estimates at fine scales. *Journal of Hydrometeorology*, *8*, 38–55. https://doi.org/10.1175/jhm560.1

Joyce, R., Janowiak, J., Arkin, P., & Xie, P. (2004). Cmorph: A method that produces global precipitation estimates from passive microwave and infrared data at high spatial and temporal resolution. *Journal of Hydrometeorology*, *5*(3), 287–296. https://doi.org/10.1175/1525-7541(2004)005<0487:camtpg>2.0.co;2

Kidd, C., Becker, A., Huffman, G. J., Muller, C. L., Joe, P., Skofronick-Jackson, G., et al. (2016). So, how much of the earth's surface is covered by rain gauges? *Bulletin of the American Meteorological Society*, *98*(1), 69–78.

Kidd, C., & Huffman, G. (2011). Global precipitation measurement. *Meteorological Applications*, *18*(3), 334–353. https://doi.org/10.1002/met.284

Kirschbaum, D., Huffman, G., Adler, R., Braun, S., & Zaitchik, B. F. (2016). NASA's remotely sensed precipitation: A reservoir for applications users. *Bulletin of the American Meteorological Society*, *98*(6), 1169–1184.

Kummerow, C., Barnes, W., Kozu, T., Shiue, J., & Simpson, J. (1998). The tropical rainfall measuring mission (TRMM) sensor package. *Journal of Atmospheric and Oceanic Technology*, *15*(3), 809–817. https://doi.org/10.1175/1520-0426(1998)015<0809:ttrmmt>2.0.co;2

Lu, H., Ding, L., Ma, Z., Li, H., Lu, T., Su, M., et al. (2020). Spatiotemporal assessments on the satellite-based precipitation products from fengyun and gpm over the yunnan-kweichow plateau, china. *Earth Space Science*, *7*, e2019EA000857. https://doi.org/10.1029/2019ea000857

Ma, Z., He, K., Tan, X., Liu, Y., Shi, Z., & Shi, Z. (2019). A new approach for obtaining precipitation estimates with a finer spatial resolution on a daily scale based on tmpa v7 data over the tibetan plateau. *International Journal of Remote Sensing*, *40*(22), 8465–8483. https://doi.org/10.1080/01431161.2019.1612118

Ma, Z., Kang, H., Xiao, T., Xu, J., Yang, H., He, Y., & Hong, Y. (2018). Comparisons of spatially downscaling TMPA and IMERG over the Tibetan Plateau. *Remote Sensing*, *10*(12), 1883. https://doi.org/10.3390/rs10121883

Ma, Z., Shi, Z., Zhou, Y., Xu, J., Yu, W., & Yang, Y. (2017). A spatial data mining algorithm for downscaling TMPA 3b43 v7 data over the Qinghai–Tibet plateau with the effects of systematic anomalies removed. *Remote Sensing of Environment*. *200*. https://doi.org/10.1016/j.rse.2017.08.023

Ma, Z., Xu, J., He, K., Han, X., & Hong, Y. (2019). An updated moving window algorithm for hourly-scale satellite precipitation downscaling: A case study in the southeast coast of china. *Journal of Hydrology*, *581*, 124378.

Ma, Z., Xu, J., Zhu, S., Yang, J., Tang, G., Yang, Y., et al. (2020). AIMERG: A New Asian Precipitation Dataset (0.1°/half-hourly, 2000–2015) by Calibrating the GPM-era IMERG at a Daily Scale Using APHRODITE. *Earth System Science Data*, *12*(3), 1525–1544. https://doi.org/10.5194/essd-12-1525-2020

Ma, Z., Xu, Y., Peng, J., Chen, Q., Wan, D., He, K., et al. (2018). Spatial and temporal precipitation patterns characterized by TRMM TMPA over the Qinghai-Tibetan plateau and surroundings. *International Journal of Remote Sensing*, *39*(12), 3891–3907. https://doi.org/10.1080/01431161.2018.1441565

Ma, Z., Zhou, L., Wu, Y., Yang, Y., & Shi, Z. (2018). Improving TMPA 3b43 v7 data sets using land-surface characteristics and ground observations on the Qinghai-Tibet plateau. *IEEE Geoence & Remote Sensing Letters*(99), 1–5. https://doi.org/10.1109/lgrs.2017.2779127

Massari, C., Brocca, L., Pellarin, T., Abramowitz, G., & Prieto, D. (2019). A daily/25 km short-latency rainfall product for data scarce regions based on the integration of the gpm imerg early run with multiple satellite soil moisture products. *Hydrology and Earth System Sciences Discussions*, *24*, 2687–2710.

Mastrantonas, N., Bhattacharya, B., Shibuo, Y., Rasmy, M., Solomatine, D., & Solomatine, D. (2019). Evaluating the benefits of merging near-real-time satellite precipitation products: A case study in the Kinu Basin region, Japan. *Journal of Hydrometeorology*, *20*(6), 1213–1233. https://doi.org/10.1175/jhm-d-18-0190.1

Sadeghi, M., Asanjan, A., Faridzad, M., Nguyen, P., Dan, B., Sorooshian, S., & Braithwaite, D. (2019). Persiann-cnn: Precipitation estimation from remotely sensed information using artificial neural networks - Convolutional neural networks. *Journal of Hydrometeorology*, *20*(12), 2273–2289. https://doi.org/10.1175/jhm-d-19-0110.1

Saha, S., Moorthi, S., Wu, X., Wang, J., Nadiga, S., Tripp, P., et al. (2014). The NCEP climate forecast system version 2. *Journal of Climate*, *27*(6), 2185–2208. https://doi.org/10.1175/jcli-d-12-00823.1

Sharifi, E., Eitzinger, J., & Dorigo, W. (2019). Performance of the state-of-the-art gridded precipitation products over mountainous terrain: A regional study over Austria. *Remote Sensing*, *11*(17), 2018. https://doi.org/10.3390/rs11172018

Sui, X., Li, Z., Ma, Z., Xu, J., Liu, H., & Liu, H. (2020). Ground validation and error sources identification for GPM IMERG product over the southeast coastal regions of china. *Remote Sensing*, *12*(24), 4154. https://doi.org/10.3390/rs12244154

Tang, G., Behrangi, A., Long, D., Li, C., & Hong, Y. (2018). Accounting for spatiotemporal errors of gauges: A critical step to evaluate gridded precipitation products. *Journal of Hydrology*, *559*, 294–306. https://doi.org/10.1016/j.jhydrol.2018.02.057

Tang, G., Clark, M., Papalexiou, S., Ma, Z., & Hong, Y. (2020). Have satellite precipitation products improved over last two decades? A comprehensive comparison of GPM IMERG with nine satellite and reanalysis datasets. *Remote Sensing of Environment*, *240*, 111697. https://doi.org/10.1016/j.rse.2020.111697

Wang, J., Hong, Y., Li, L., Gourley, J. J., Khan, S. I., Yilmaz, K. K., et al. (2011). The coupled routing and excess storage (CREST) distributed hydrological model. *Hydrological Sciences Journal*, *56*(1), 84–98. https://doi.org/10.1080/02626667.2010.543087

Wang, Q., Wu, X., Chen, Y., & Duan, J. (2019). Visualization and Application of FY-4A Satellite Data. *Meteorol. Ence Technol.*, *3*, 502–507.

Xie, Y., Lin, K., Yang, S., & Lin, R. (2013). IEEE. Study on spatial-temporal distribution and tendency variation characteristics of annual precipitation in Jiangxi Province. *2013 IEEE Third International Conference on Information Science and Technology (ICIST)*.

Xu, J., Ma, Z., Tang, G., Ji, Q., Min, X., Wan, W., & Shi, Z. (2019). Quantitative evaluations and error source analysis of Fengyun-2-based and GPM-based precipitation products over mainland China in summer, 2018. *Remote Sensing*, *11*(24), 2992. https://doi.org/10.3390/rs11242992

Xu, L., Zhu, M., He, B., Wang, X., Zhang, Q., Jiang, J., & Razafindrabe, B. H. N. (2014). Analysis of water balance in Poyang Lake basin and subsequent response to climate change. *Journal of Coastal Research*, *68*, 136–143. https://doi.org/10.2112/si68-018.1

Yu, C., Hu, D., Liu, M., Wang, S., & Di, Y. (2020). Spatio-temporal accuracy evaluation of three high-resolution satellite precipitation products in China area. *Atmospheric Research*, *241*, 104952. https://doi.org/10.1016/j.atmosres.2020.104952

Zhang, Q., Xiao, M., Singh, V. P., & Wang, Y. (2016). Spatiotemporal variations of temperature and precipitation extremes in the Poyang Lake Basin, China. *Theoretical and Applied Climatology*, *124*, p 855–864. https://doi.org/10.1007/s00704-015-1470-6

Zhu, S., Shen, Y., & Ma, Z. (2020). A new perspective for charactering the spatio-temporal patterns of the error in GPM IMERG over mainland China. *Earth and Space Science*, *8*(1), 29–35.